



**HAL**  
open science

## Video sensor node energy preservation through dynamic adaptive video encoding parameters' values selection

Othmane Alaoui-Fdili, François-Xavier Coudoux, Youssef Fakhri, Patrick Corlay, Driss Aboutajdine

### ► To cite this version:

Othmane Alaoui-Fdili, François-Xavier Coudoux, Youssef Fakhri, Patrick Corlay, Driss Aboutajdine. Video sensor node energy preservation through dynamic adaptive video encoding parameters' values selection. *Sustainable Computing: Informatics and Systems*, 2018, 18, pp.34-44. 10.1016/j.suscom.2018.02.006 . hal-03183506

**HAL Id: hal-03183506**

**<https://hal.science/hal-03183506>**

Submitted on 12 Jun 2024

**HAL** is a multi-disciplinary open access archive for the deposit and dissemination of scientific research documents, whether they are published or not. The documents may come from teaching and research institutions in France or abroad, or from public or private research centers.

L'archive ouverte pluridisciplinaire **HAL**, est destinée au dépôt et à la diffusion de documents scientifiques de niveau recherche, publiés ou non, émanant des établissements d'enseignement et de recherche français ou étrangers, des laboratoires publics ou privés.

# Video sensor node energy preservation through dynamic adaptive video encoding parameters' values selection

Othmane Alaoui-Fdili <sup>a,d,\*</sup>, François-Xavier Coudoux <sup>b</sup>, Youssef Fakhri <sup>c</sup>, Patrick Corlay <sup>b</sup>, Driss Aboutajdine <sup>d</sup>

<sup>a</sup> LAPSSII, Ecole Supérieure de Technologie de Safi, Université Cadi Ayyad, Safi, Morocco

<sup>b</sup> Univ. Valenciennes, CNRS, Univ. Lille, YNCREA, Centrale Lille, UMR 8520 – IEMN, DOAE, 59313 Valenciennes, France

<sup>c</sup> LARIT équipe réseaux et Télécommunications, Ibn Tofail University, Kénitra, Morocco

<sup>d</sup> LRIT-CNRST URAC29, Faculty of Sciences, Mohammed V University in Rabat, Morocco

## Article Info

### Keywords:

Energy consumption

Adaptive video encoding

H.264/AVC

Intra coding

Lifetime extension

Wireless videos sensor networks

## Abstract

Wireless video sensor networks (WVSN) are energy constrained systems where deployed video nodes are capable of capturing the visual scene, performing local processing such as video compression, then routing the results toward the destination. In this paper, we consider the problem of minimizing the energy consumed by the video sensor node to encode and transmit the video stream under a defined video quality constraint. In the present work, Intra-Only H.264/AVC is considered as video compression scheme. Particularly, we propose to control at run-time both the energies consumed for video encoding and transmitting, in addition to the video encoding distortion. Thus, we begin our study by profiling the evolution of these quantities according to two coding parameters, namely the frame rate (FR) and the quantization parameter (QP). Following an analysis of the obtained measurements, we propose empirical parametric models in line with the observed behaviors, then validate them with different video sequences. Finally, we introduce the Dynamic Adaptive Encoding Parameters' values Selection (DAEPS) procedure which relies on these models to solve the problem under consideration. Simulations show the advantage of considering such an approach, which is capable, on the one hand, of extending the lifetime of the video sensor node up to 2.3 times, when compared with state-of-the-art approaches, and on the other hand, of complying with the defined end-to-end video quality constraint.

## 1. Introduction

Wireless sensor networks (WSN) are offering a new solution for monitoring indoor and outdoor environments [1,2]. They consist of a large number of interconnected sensor nodes, and can collect data, process, then route them towards the destination using multi-hops short range transmissions. Sensor nodes are battery powered units and replacing this component is in general difficult, and in some cases, impossible. Therefore, all possible efforts have been made to propose energy-efficient communication algorithms and schemes in order to extend node lifetime as much as possible [3,4]. The recent advances in CMOS image and video processing technologies have allowed the sensor nodes to capture and process visual information. Networks of such interconnected devices are

called Wireless Video Sensor Networks (WVSN)s [5,6]. Recently, the research in WVSNs gained high interest due to the multitude of applications that are envisioned and could be developed [7].

In a WVSN, the collected visual information needs to be compressed prior to transmission. Hence, new challenges have been introduced to the WSN researchers community because of the particular features of this kind of data. Specifically, processing energy was so far neglected in WSNs since it was considered a very simple operation [2]. However, the energy consumed for video data processing has to be taken into account [8]. According to the experiments presented in [9], conducted on Stargate/Telos video sensor nodes, the computational energy depletion constitutes the major portion (more than 90%) of the total energy consumption compared to the bit transmission energy. Therefore, energy-efficient compression schemes are needed since a large amount of energy is drained during this phase.

The particularity of the context of the WVSN suggests designing more adaptive solutions, that consider at every stage the various indicators reflecting the current state of the node and its neighbor-

\* Corresponding author at: LAPSSII, Ecole Supérieure de Technologie de Safi, Université Cadi Ayyad, Safi, Morocco.

E-mail address: [othmane.alaoui.fdili@gmail.com](mailto:othmane.alaoui.fdili@gmail.com) (O. Alaoui-Fdili).

hood. In this paper, the considered indicators are the remaining energy (RE) of the video source node as well as the perceived transmission distortion. The key idea of the paper is to propose an energy-efficient and adaptive video encoding scheme that, given a user's end-to-end desired video quality, an estimated transmission distortion and a current remaining energy budget, selects the appropriate configuration in terms of the quantization parameter (QP) and frame rate (FR) to preserve from useless energy consumption while meeting the specified desired end-to-end video quality. The considered video encoding standard is the Intra-only H.264/AVC in its Baseline profile [10]. Practically, to reach our objective, we first investigate the behavior of the considered energies and distortion. Then, we propose empirical parametric models, as functions of QP and FR, in line with the observed behaviors. Third, the proposed models are validated using a different set of video sequences. Finally, we introduce the dynamic adaptive encoding parameters' values selection (DAEPS) procedure, which relies on these to perform energy saving while meeting the required end-to-end video quality.

The choice of the Intra-only prediction mode is motivated by the results of the experiments presented in [9,11], showing that inter-coding consumes more than 10 times the energy drained by Intra-coding. Hence, choosing Intra-only coding significantly limits the energy consumption of the resource-limited video nodes. It might indeed be expected that the Intra-only coding results in lower compression ratio, but the use of reduced frame rate compensates for this. Furthermore, Intra-only coding avoids error propagation across successive frames, hence preserving video quality. Our motivations behind the choice of QP and FR as controlling parameters in this work are twofold: first, the QP and FR parameters are used in all video encoding standards. Second, they are easy to access on different industrial cameras, such as the LILIN IPD2220ES [12], offering controllable multiple FR and bit rates (i.e., QP). Consequently, the present proposition could be adapted for further standards and easily used by existing cameras or prototyped ones in order to extend their lifetime when used in an energy-constrained system. An extension of this work to the case of ROI-oriented robust transmission, using three video encoding parameters, in addition to an interactive original routing protocol, with node and network levels evaluations, has been recently accepted for publication in [13].

The rest of this paper is organized as follows: Section 2 presents a review of the relevant approaches for sensor node lifetime extension. In Section 3, the main contributions of this paper are explained in detail. Section 4 validates the proposed models then applies the proposed DAEPS procedure. Finally, Section 5 concludes the paper.

## 2. Related works

Due to the inherent features of the WSNs, which are known as energy-constrained systems, many works have addressed the problem of network lifetime extension under the quality of service constraints. In a typical WSN, with only scalar data, the energy conservation is mainly performed only in the lower layers of the protocol stack, namely the network, MAC and physical layers. For instance, to decrease the energy consumed by idle listening, where a node listens for any possible incoming packets, many works have adopted the technique of duty cycling as a solution [14]. In fact, in [15], the authors introduced the FTA-MAC protocol consisting of rapid adaptation of the receiving nodes wakeup interval according to the source nodes sending rate, which leads to a reduction of the receiving nodes idle listening. Moreover, since the ISM bands are often crowded, the sensor node may decide to wake up upon false detections of surrounding WiFi transmissions. This false wakeup causes significant waste of energy. As a solution, the authors in [16]

proposed the Adaptive Energy Detection Protocol, an application-oriented protocol which is able to dynamically adjust a nodes wakeup threshold to improve network reliability and duty cycle. Energy efficiency could also be performed at the PHY layer by optimizing modulation sizes and/or transmission durations in order to minimize the total energy consumption, for example. This particular idea was investigated in [17], which focused on Gaussian channels subject to the delay and peak power constraints, and in [18], which considered fading channels subject to the bit-error-rate (BER) constraints. On the other hand, the authors of [19] adopted the adaptive power allocation idea to achieve network lifetime extension. In fact, instead of transmitting at a fixed power, this last could be adapted with respect to the observed signal to noise ratio (SNR) for more energy saving. Other energy-efficient techniques performed at the MAC and PHY layer, such as unequal protection and retransmission, the distributed beamforming, contention free techniques and the cross-layer design, are listed in surveys [20–22].

Routing is an additional energy consuming phase. To decrease its energy consumption, many solutions could be adopted. One of the most popular is using cluster architecture [23], consisting of subdividing the network into clusters, where each one is managed by a selected node known as the Cluster Head (CH). The CH node is responsible of coordinating the members duty cycles, communications, and performing data aggregation. Thanks to this architecture, the communication and the number of transmissions are reduced, as is the consumed energy. This idea was adopted in several works and proved its ability to decrease the consumed energy over the network [24]. Another way to enhance energy efficiency during the routing process is to consider the remaining energy of the intermediate nodes as a metric in the setup path phase. In fact, the proposed routing protocol in [25] considered this information to establish the next hops candidates scores. The simulation results demonstrated that taking into account the residual energy of the forwarding nodes could notably extend the sensor nodes' lifetime while meeting the quality of service requirements. Other techniques for performing energy-efficient routing are highlighted in [26].

The introduction of visual information in the WSNs has prompted researchers to think of more solutions to realize further energy efficiency. Since the energy consumed during the video/image processing, prior to transmission, is considerable, several works have focused on the introduction of energy efficiency during the video/image compression phase [27,28]. In [29], the authors present a solution based on the correlation characteristics of visual information in the sensor networks. In fact, energy efficiency is achieved using a correlation-aware inter-node differential coding scheme conducted by the H.264/ MVC video coding standard. Using the multiview concept, redundant data of overlapping fields of views are encoded once.

In [30], the authors propose an energy-efficient and adaptive video compression scheme dedicated to the WWSN. The energy efficiency comes from the adoption of two modes, namely the standby and the rush modes, conditioned by a low and high FR respectively. In addition, a simple bit rate adaptation technique, called the frequency selectivity (FS), is applied to the region of interest (ROI) and the background (BKGD) respectively, in order to separately adjust the bit rate of each scene area, hence decreasing the energy consumed during the transmission process. However, the consumed energy during the encoding process was not considered and the selection of the encoding parameters' values -particularly the FR and the QP- was done in a static manner.

Lately, the idea of adapting the video encoding parameters' values at run-time has been gaining more interest in the WWSN context. An adaptive cross-layer framework for video transmission over the WSNs (ACWSN) is presented in [31] and used in [32]. ACWSN adapts the video encoding parameters, namely the group of pictures (GOP) length (i.e.,  $G_L$ ) and the number of  $B$  frames (i.e.,

$B_f$ ), depending on the current wireless channel state, for maximizing only the video quality in terms of PSNR. The authors prove through experiments that the GOP structure, if chosen properly within given intervals, could decrease the perceived video distortion. The authors of [33] present a study concerning the appropriate parameters' values for an optimal complexity of the H.264/AVC video encoding standards in the wireless multimedia sensor network (WMSN) context. In fact, through an analytic study, only the H.264/AVC encoder energy consumption is expressed as a function of the search range (SR) and number of reference frames (NRF) parameters. In comparison to these particular works, we address, in this paper, the problem of decreasing both the encoding and transmission energy consumption while considering a specified video quality constraint. Furthermore, we are considering other encoding parameters affecting the energy consumption as well as the video quality, which are the QP and the FR.

### 3. Description of the proposed DAEPS-based video encoder

The aim of this section is to describe the proposed energy efficient video encoder and the different steps towards its establishment. Recall the main objective of this work is to enable the video encoder to automatically select the optimal configuration in terms of QP and FR to meet the desired end-to-end video quality on one hand, and on the other hand, to minimize as much as possible the consumed energy to reach that quality.

Before going any further, let us see what the video stream is experiencing from the capture till the reception. When an event occurs, the concerned video sensor node starts capturing the scene. Prior to the transmission, the video stream is compressed according to a given video compression algorithm or standard under a given configuration. Here, an encoding energy (EE) is drained and a first distortion of the original signal is observed, namely, the encoding distortion (ED). The encoded stream is then packetized and routed to the destination via multihops short-range transmissions. Here, a transmission energy (TE) is consumed by the video sensor node to transmit the video stream to the next hop, and a second distortion, namely the transmission distortion (TD), is observed. In summary, with respect to the considered controlling parameters, the total energy (E) and distortion (D) could be formulated as follows:

$$E(QP, FR) = EE(QP, FR) + TE(QP, FR) \quad (1)$$

$$D(QP, FR, PLR) = ED(QP, FR) + TD(PLR) \quad (2)$$

where PLR refers to the estimated packet loss rate (PLR) responsible for the transmission distortion.

The proposed video encoder selects the video encoding parameters, QP and FR, with respect to the observed transmission distortion and the remaining energy of the node. In fact, the selected QP and FR are expected to offer a total distortion that does not exceed the specified one while consuming a minimal total energy  $E(QP, FR)$ . Therefore, we need to first derive empirical models describing the behavior of the consumed energies and the observed distortions. Then, the dynamic adaptive encoding parameters' values selection (DAEPS) procedure that uses these models will be exposed.

#### 3.1. Energy and distortion modelling

We adopt an operational approach for offline energy consumption and distortion analysis and modelling, which can be applied to generic video encoders. It consists of a consideration of the parameters that are responsible for consuming more or less energy and altering the video quality during the video signal compression and transmission [11]. In the following, we profile the impact of FR and QP variations on the consumed energy as well as the occurred dis-

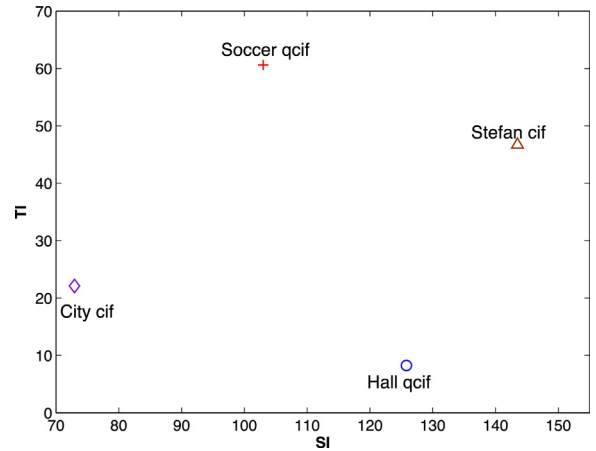


Fig. 1. The coverage of the considered video sequences over the spatial-temporal information plane.

ortion. It is expected that the energy consumption decreases when the QP increases and the FR decreases. On the other hand, it is also expected that the distortion increases when the QP increases. However, the question that we wish to answer is: how do the distortion and energy behave exactly with respect to QP and FR, and specifically when Intra-only coding is used?

In order to derive appropriate models, extensive tests were carried out for measurements using several video sequences. The ITU-T [34] recommends the selection of appropriate video sequences to consider the spatial and temporal perceptual information of the scenes, defined in [34] and noted in the following SI and TI respectively. In fact, these parameters reflect the compression difficulty as well as the level of impairment that is suffered when the scene is transmitted. Furthermore, it is important to choose sequences that span a large portion of the spatial-temporal information plane [34]. Therefore, we use four video sequences, Hall and Soccer in QCIF resolution ( $176 \times 144$ ), City and Stefan in CIF resolution ( $352 \times 288$ ). Fig. 1 illustrates the distribution of the chosen video sequences over the spatial-temporal information plane. As can be seen, the considered set of sequences covers a large area, showing its SI-TI diversity. In fact, according to Fig. 1, this set includes video sequences representing contents with a moderate TI and SI ranging from low to high (i.e., City and Stefan), while others represent contents with a moderate SI and TI ranging from low to high (i.e., Soccer and Hall).

##### 3.1.1. Energy consumption analysis and modelling

In [11], the impact of FR and QP variations on only the encoding energy consumption of an Intra-only H.264/AVC encoder is addressed, and for only QCIF video sequences. In the following, we extend the study presented in [11] by including CIF video sequences and investigating the impact of the FR and QP variations on both encoding and transmission energy consumption.

##### (a) Encoding energy (EE) as function of QP:

The consumed energy for processing can be modelled as presented in [29] as a function of the number of clock cycles by:

$$E_{Proc}(N) = N_{cyc} \cdot C_{total} \cdot V_{dd}^2 + V_{dd} \cdot (I_0 e^{\frac{V_{dd}}{nV_T}}) \cdot \left( \frac{N_{cyc}}{f} \right) \quad (3)$$

where  $N_{cyc}$  is the number of clock cycles,  $C_{total}$  is the average capacitance switched per cycle,  $V_{dd}$  is the supply voltage,  $I_0$  is the leakage current,  $f$  is the clock speed,  $V_T$  is the thermal voltage and  $n$  a processor dependent constant. On the other hand, since:

$$T_{Proc} = \frac{N_{cyc}}{f} \quad (4)$$

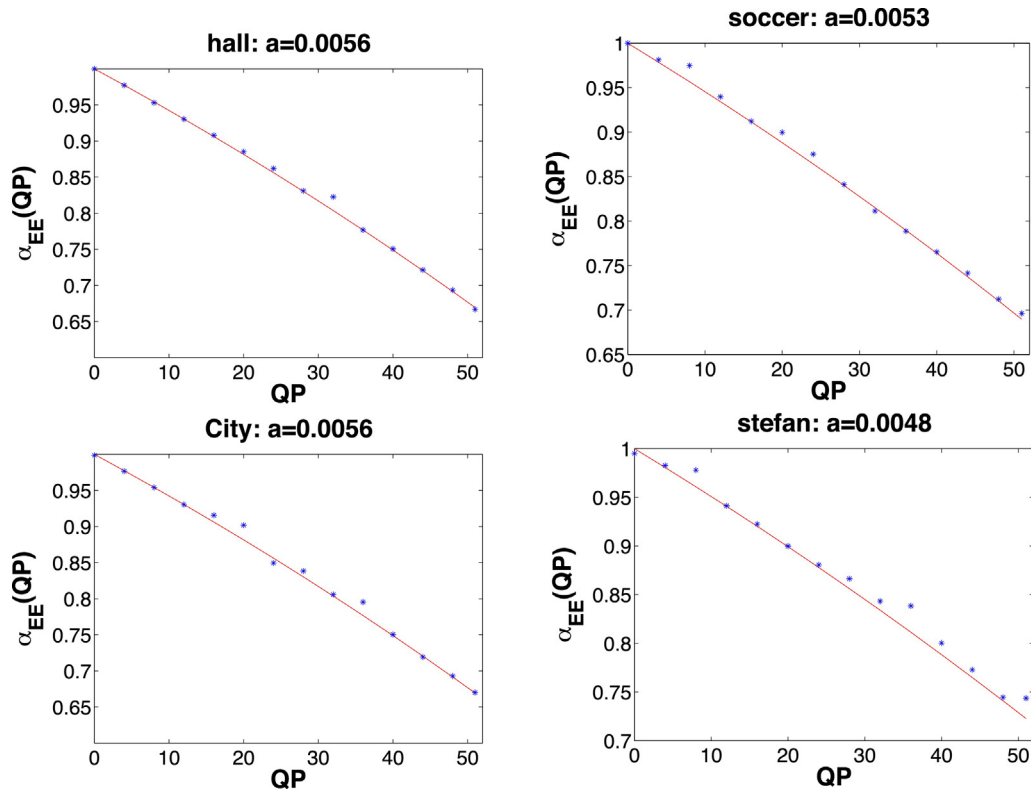


Fig. 2. Measured (points) and predicted (curves)  $\alpha_{EE}(QP)$ . Curves are predicted values by the proposed model of Eq. (7).

then,

$$N_{cyc} = T_{Proc} \quad (5)$$

where  $T_{Proc}$  is the processing time, which is the encoding time in our case returned by the encoder.

The measured  $T_{Proc}$  in our case, is the sum of four major sub-tasks and hence can be written as follows:

$$T_{Proc} = T_{IP} + T_T + T_Q + T_{EC} \quad (6)$$

where  $T_{IP}$  is the intra prediction time,  $T_T$  is the  $4 \times 4$  DCT integer transform time,  $T_Q$  is the time for the quantization operation and  $T_{EC}$  is the time for the CAVLC entropy coding.

For reliable and accurate measurements, we control the running of the encoder to be in a real-time fashion and make it the only executed process in one microprocessor. Once the measurements are converted to energies, using the model of Eq. (3), they are normalized by the maximal consumed energy.

Points in Fig. 2 report the measured  $\alpha_{EE}(QP)$  that expresses the effect of the quantization on the normalized consumed energy during the encoding process. We can notice that the energy decreases slowly when the QP is increased. This can be explained by increasing the QP, when the quantization becomes more severe, generating macroblocks with more zero quantized coefficients. This result reduces the energy consumed during the CAVLC entropy coding. Fig. 2 shows the behavior of a reduction factor that is QP-dependent. This factor reaches its maximum value of 1 at  $QP = QP_{min} = 0$ , then slowly decreases while the QP increases. Based on the above mentioned arguments, we propose to model  $\alpha_{EE}(\cdot)$  as follows:

$$\alpha_{EE}(QP) = 2 - e^{-(a \cdot QP)} \quad (7)$$

where  $a$  is a content dependent coefficient. As shown in Fig. 2, the proposed model in Eq. (7) can predict the reduction coefficients  $\alpha_{EE}(\cdot)$  accurately with an average RMSE of 6%.

(b) Transmission energy (TE) as function of QP:

The energy consumed per bit during the transmission process is given by the well-known model proposed in [23]:

$$E_{Tx} = E_{elec} + \epsilon_{fs} \cdot d^2 \quad (8)$$

where  $\epsilon_{fs}$  is the energy consumed by the amplifier to transmit at short distance,  $E_{elec}$  is the energy dissipated in the electronic circuit to transmit and receive the signal, and  $d$  is the distance between the transmitter and the receiver. The path loss exponent is set to 2. This value is quite reasonable for free space propagation model, which is characteristics of most WSN applications. Based on this model, the energy consumed for transmitting, at a given distance  $d$  at a fixed  $\epsilon_{fs}$  and  $E_{elec}$ , depends directly of the data rate generated by the encoder.

Points in Fig. 3 report the measured  $\alpha_{TE}(QP)$ , representing the effect of the quantization on the normalized consumed energy during the transmission process. As can be seen,  $\alpha_{TE}(\cdot)$ , similar to  $\alpha_{EE}(\cdot)$  reaches its maximum at  $QP = QP_{min}$  and its minimum at  $QP = QP_{max}$ . However,  $\alpha_{TE}(\cdot)$  decreases faster than  $\alpha_{EE}(\cdot)$  and reaches minimal values approaching 0. Therefore, we propose to model  $\alpha_{TE}(\cdot)$  as an exponentially decreasing function of QP, as follows:

$$\alpha_{TE}(QP) = e^{-k \cdot QP} \quad (9)$$

where  $k$  is a content-dependent coefficient obtained by minimizing the RMSE between measured and predicted data. As shown in Fig. 3, the proposed model given by Eq. (9) can predict the reduction coefficients  $\alpha_{TE}(\cdot)$  accurately with an average RMSE of 4%.

(c) Impact of FR variation on EE and TE:

The FR is the second factor that we consider to predict the energy consumption of our video encoder. We can change the FR in the JM implementation of H.264/AVC by varying the parameter Frame

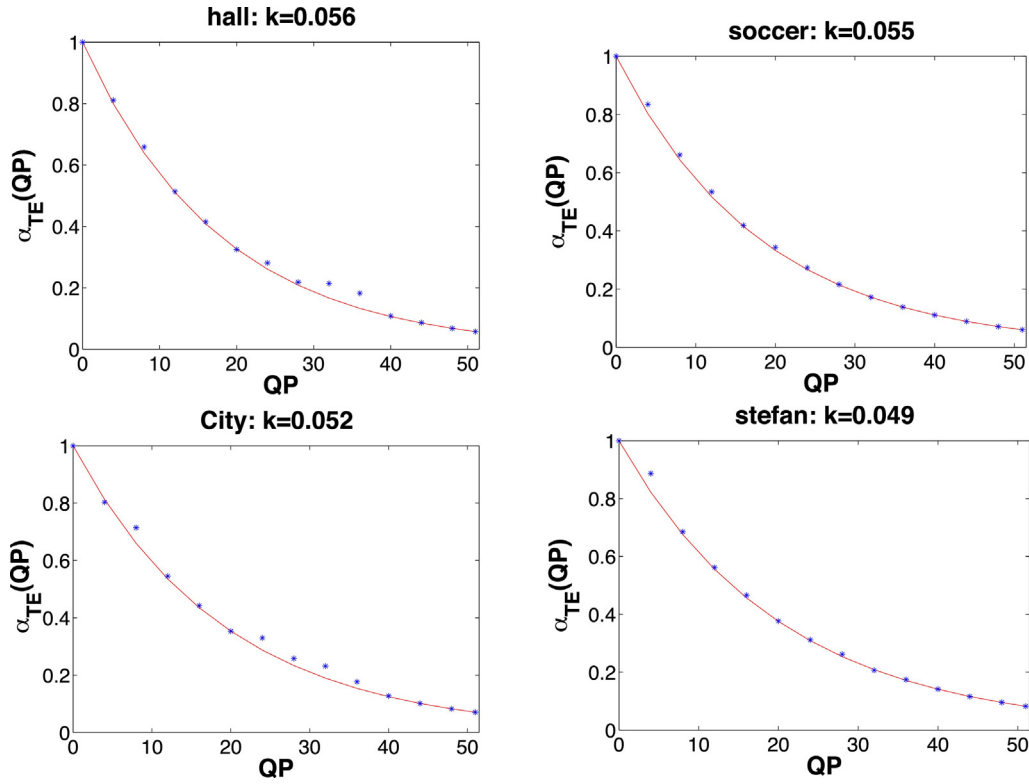


Fig. 3. Measured (points) and predicted (curves)  $\alpha_{TE}(QP)$ . Curves are predicted values by the proposed model of Eq. (9).

Skip (FSkip). The relation between these two parameters is given as follows:

$$FSkip = \left\lceil \frac{FR_{max}}{FR} \right\rceil - 1 \quad (10)$$

where  $FR_{max}$  is the maximal FR allowed.

Points in Figs. 4 and 5 present the measured normalized energy, for encoding and transmission respectively, while varying the FSkip. As can be seen, the impact of the FSkip parameter on the encoding and transmission energies is the same. In fact, the energy consumed decreases when increasing the FSkip and thus decreasing the FR. This can obviously be explained by reducing the FR, when the FSkip is increased and hence, less frames are encoded and transmitted, leading to a considerable reduction of the consumed energy. Note that the  $FR_{max}$  of the tested video sequences is 30 fps, and using Eq. (10), one can deduce the tested FRs. Also, we notice that an increment of the FSkip by 1 reduces the energy by about half and so on, which is an obvious and expected behavior.

Points in Figs. 4 and 5 show the behavior of a reduction factor that is FSkip-dependent. We name it  $\gamma(FSkip)$ . This factor reaches its maximum value of 1 at  $FSkip = FSkip_{min} = 0$  and quickly decreases to its minimal value at  $FSkip = FSkip_{max} = 29$ . In addition, this factor does not attain the zero value since there is at least one frame to be encoded. Based on the above mentioned arguments, we propose to model  $\beta(\cdot)$  as follows:

$$\gamma(FSkip) = \frac{1}{2^{FSkip}} + b \quad (11)$$

where  $b$  is a content dependent parameter. As can be seen, the proposed simple model of Eq. (11) is able to predict the coefficients  $\gamma(\cdot)$  with an average RMSE of 7%. Other analytical expressions, such as  $\frac{1}{1+FSkip} + b$  or  $\frac{1}{b*FSkip+1}$  would lead to an enhancement of 3% in terms of RMSE. However, they do not reflect immediately the above-mentioned physical reality of the FSkip parameters impact on the consumed energy (i.e., the reduction by about the half).

(d) Global models as functions of QP and FR:

The maximal energy consumed during the video signal encoding and transmission is reduced by a QP-dependent reduction coefficient, then by a FR-dependent reduction coefficient. Hence, the global model for predicting the consumed energy during the video signal encoding is given by:

$$EE(QP, FR) = EE(QP_{min}, FR_{max}) \cdot \alpha_{EE}(QP) \cdot \gamma\left(\left\lceil \frac{FR_{max}}{FR} \right\rceil - 1\right) \quad (12)$$

where  $EE(QP_{min}, FR_{max})$  is the maximum energy consumed during the video signal compression, corresponding to the pair  $(QP_{min}, FR_{max})$ .

The global model for predicting the consumed energy during the video signal transmission is given by:

$$TE(QP, FR) = TE(QP_{min}, FR_{max}) \cdot \alpha_{TE}(QP) \cdot \gamma\left(\left\lceil \frac{FR_{max}}{FR} \right\rceil - 1\right) \quad (13)$$

where  $TE(QP_{min}, FR_{max})$  is the maximum energy consumed during the video signal transmission, corresponding to the pair  $(QP_{min}, FR_{max})$ .

### 3.1.2. Distortion analysis and modelling

In the following, we derive a model for video encoding distortion (ED) prediction. Note that the distortion is expressed in terms of mean squared error (MSE), and is given by:

$$MSE(X, Y) = \frac{\sum_{i=1, j=1}^{m, n} (X_{i,j} - Y_{i,j})^2}{m \cdot n} \quad (14)$$

where  $X$  is the frame of original video sequence,  $Y$  is the frame of compressed or received video sequence, and  $m$  and  $n$  are frame width and height respectively. In what follows, as a first approach, only the distortion due to the quantization process is considered. The impact of FR variations on the perceived video quality will be accounted for in a further study.

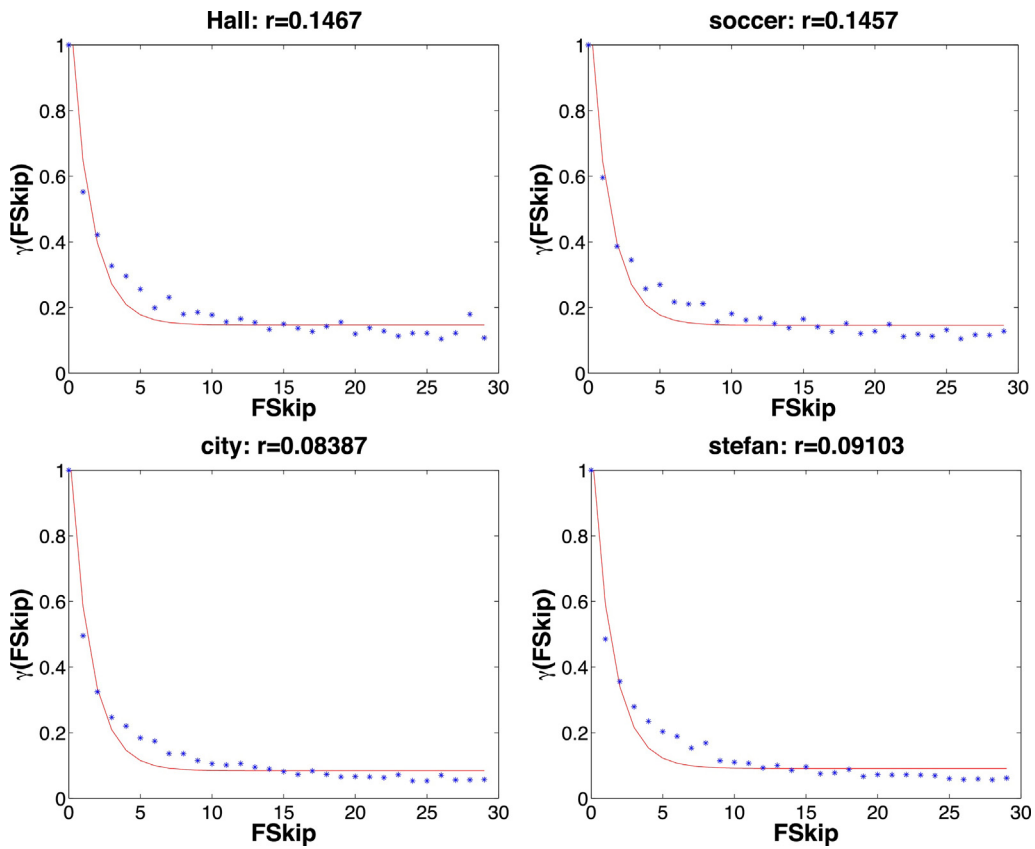


Fig. 4. Measured (points) and predicted (curves)  $\gamma(\text{FSkip})$  for the encoding. Curves are predicted values by the proposed model of Eq. (11).

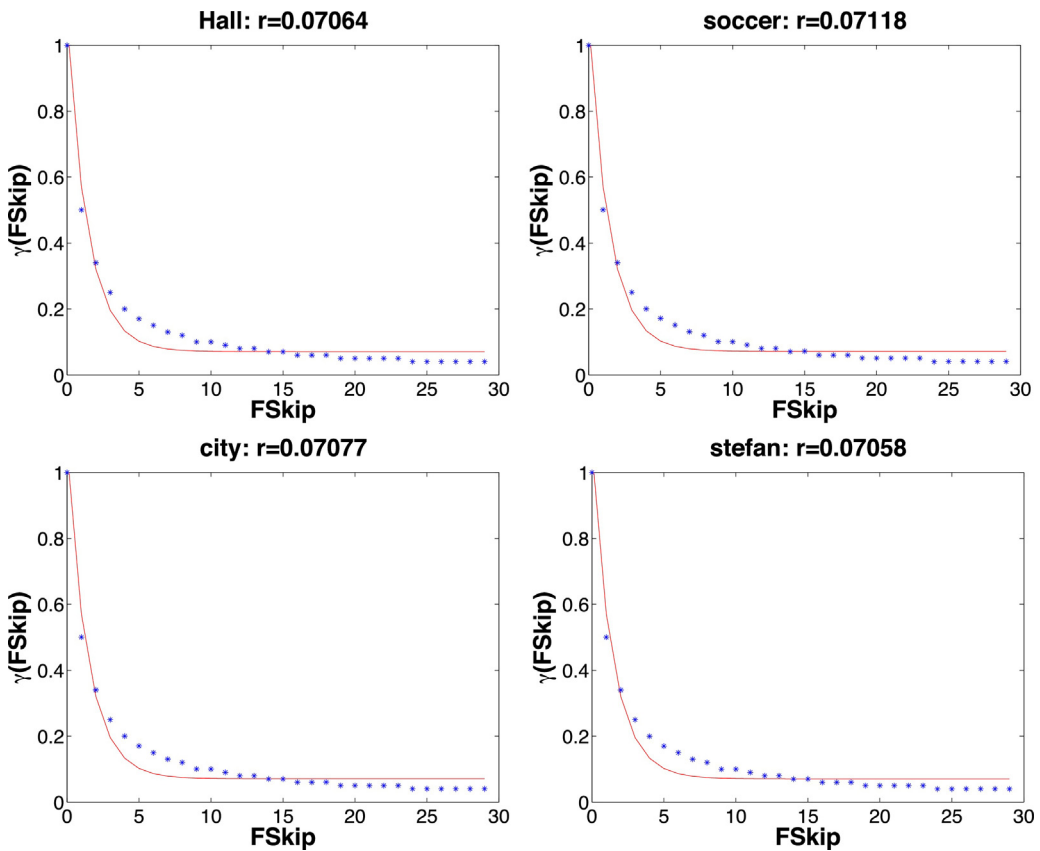


Fig. 5. Measured (points) and predicted (curves)  $\gamma(\text{FSkip})$  for the transmission. Curves are predicted values by the proposed model of Eq. (11).

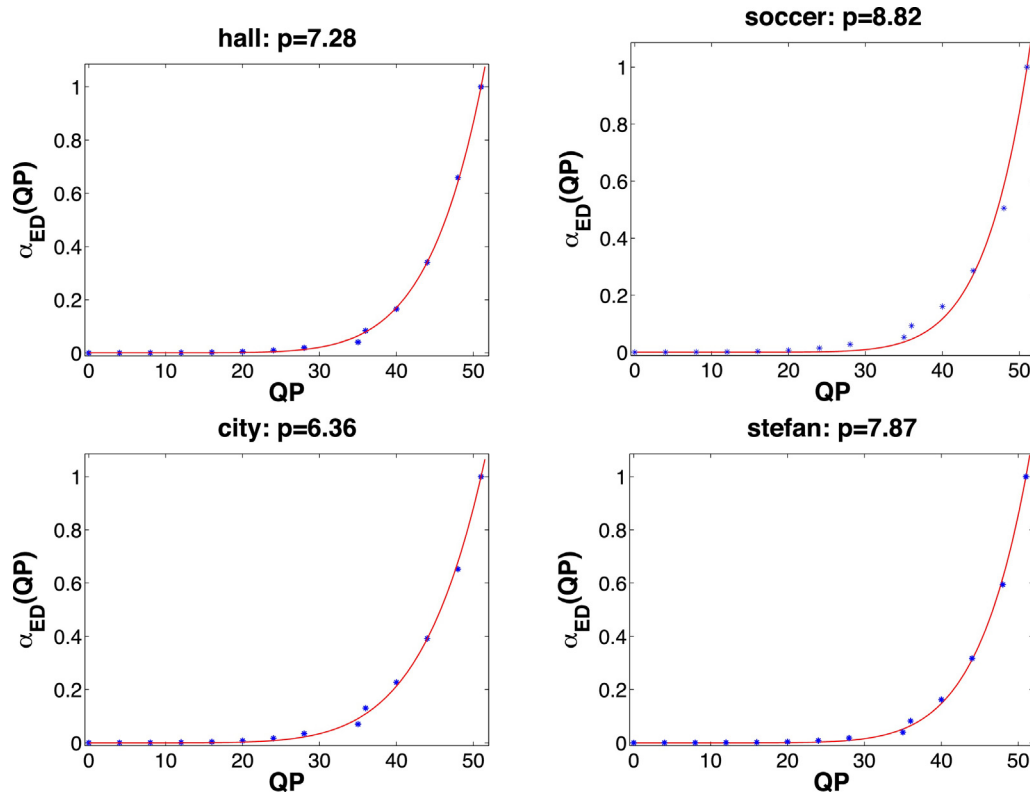


Fig. 6. Measured (points) and predicted (curves)  $\alpha_{ED}(QP)$ . Curves are predicted values by the proposed model of Eq. (15).

The distortion introduced by the encoding process can be expressed as a function of the QP. Points in Fig. 6 report the normalized measured encoding distortion. Unlike the encoding energy, increasing the QP leads to an increase of the video distortion, which is an obvious behavior. In fact, when the quantization is severe, more relevant information is lost. This directly affects the measured quality that drops dramatically. Note that the normalization is done by the maximal encoding distortion value, reached for  $QP_{max}$ .

Points in Fig. 6 report the measured  $\alpha_{ED}(QP)$ , containing the effect of the quantization on the normalized distortion caused by the encoding process. Unlike  $\alpha_{EE}(\cdot)$ ,  $\alpha_{ED}(\cdot)$  reaches its maximum at  $QP=QP_{max}$  and its minimum at  $QP=QP_{min}$ . In addition,  $\alpha_{ED}(\cdot)$  observes a quasi-stationary phase until a given QP is reached, where  $\alpha_{ED}(\cdot)$  sharply increases. Therefore, we propose to model  $\alpha_{ED}(\cdot)$  by:

$$\alpha_{ED}(QP) = \left( \frac{QP}{QP_{max}} \right)^p \quad (15)$$

where  $p$  is a content-dependent coefficient obtained by minimizing the RMSE between measured and predicted data. As shown in Fig. 6, the proposed model in Eq. (15) can predict the reduction coefficients  $\alpha_{ED}(QP)$  accurately with an average RMSE of 4%.

Finally, the proposed model for encoding distortion prediction as function of QP is as follows:

$$ED(QP) = ED(QP_{max}) \cdot \alpha_{ED}(QP) \quad (16)$$

where  $ED(QP_{max})$  is the maximum encoding distortion measured for  $QP_{max}$ .

The introduced transmission distortion is mainly dependent on the adopted encoding methodology (e.g., inter or intra) as well as the PLR. In our case, since Intra-only encoding is performed, there is no temporal errors propagation. Therefore, for a given PLR, the observed transmission distortion could be predicted by a model such as proposed in [35] as follows:

$$PSNR(PLR) = \lambda \cdot \ln(1 - PLR) + \mu \quad (17)$$

where  $\lambda$  and  $\mu$  model parameters.

Note that in this paper, the considered PLRs are those concerning the video data packets. Finally, knowing the following relation, the transmission distortion could be deduced in terms of MSE:

$$PSNR = 10 \log_{10} \left( \frac{255^2}{MSE} \right) \text{ dB} \quad (18)$$

considering images are coded on one byte per pixel.

### 3.2. Dynamic adaptive encoding parameters' values selection (DAEPS) procedure

In this section, we explain how the above presented models perform the dynamic adaptive encoding parameters' values selection (DAEPS), and hence improve energy efficiency while meeting the desired video quality. The flowchart of Fig. 7 gives a detailed step-by-step execution of the DAEPS procedure. As inputs, this procedure considers the user's video distortion constraint, the node's remaining energy, the observed PLR, a range of allowed FRs  $[FR_{min}, FR_{max}]$  and allowed QPs  $[QP_{min}, QP_{max}]$ . When a video node needs to encode and transmit a video stream according to the DAEPS procedure, the following steps are executed:

#### Step 1: Determination of the QPs satisfying the video quality constraint

Given the PLR, the node could approach the transmission video distortion using the model in Eq. (17). Consequently, using Eq. (2), the allowed encoding distortion is deduced. Afterwards, thanks to the encoding distortion model of Eq. (16), a solution set of QPs, satisfying the encoding distortion constraint is constructed.

#### Step 2: Determination of the pair (QP,FR) minimizing the energy consumption

First, the FR is initialized at  $FR_{max}$ . Then, each pair (QP,FR) is evaluated in terms of energy consumption using the models of Eqs. (12) and (13) for predicting the encoding and transmitting con-

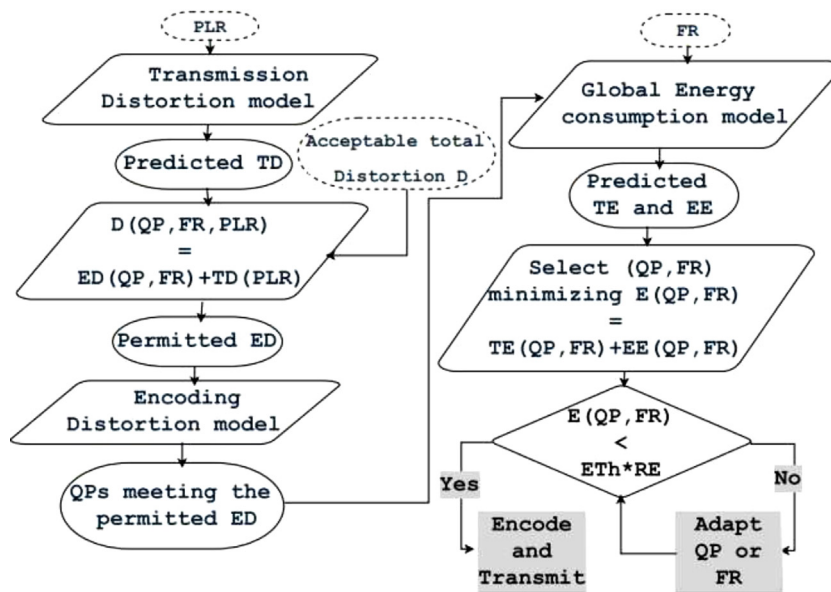


Fig. 7. DAEPS procedure's flowchart.  $E_{Th}$  is the energy threshold discussed in Step 3.

**Table 1**  
SI and TI of the considered sequences for the models validation.

	Bus	News	Ice	Foreman
SI	149.8	126.8	118.7	105.6
TI	38.3	30.3	28.7	35.8

sumed energies respectively. Afterwards, the video encoder selects the pair minimizing the energy consumption.

**Step 3: Checking the feasibility of the encoding and transmitting**

On the basis of the estimated total energy consumption of the selected configuration, the video encoder decides whether or not it could compress and transmit the stream. If the node's remaining energy is greater than the required energy for encoding, then transmitting using the selected pair by a given threshold, the energy threshold ( $E_{Th}$ ), the node may encode the video stream and relay it to the network layer.

Whenever the remaining energy is insufficient for encoding and transmitting the video stream, the video encoder performs the Adapt and reevaluate step.

**Step 4: Adapt and reevaluate**

The video encoder decreases the adopted  $FR$  and goes to Step 2. If the lower permitted  $FR_{min}$  is reached, and the node is still incapable of encoding and transmitting due to lack of energy, the video encoder increases the selected  $QP$ , then goes to Step 3 to check the feasibility of the encoding and transmitting until the maximal permitted  $QP_{max}$  is attained.

Finally, if the node is still incapable of performing the encoding and the transmission, it turns off the video module and remains as a relaying node. This is done to prevent holes in the network's topology that degrade the quality of service.

**4. Models validation and application of the DAEPS procedure**

**4.1. Models validation**

In this section, we validate the proposed models using another set of video sequences: Bus and News in CIF resolution, Ice and Foreman in QCIF resolution. Table 1 reports the pairs (SI, TI) of each considered sequence. Since the parameters of the proposed models

are content dependent, we propose, as a first approach, to select the models parameters' values on the basis of the (SI, TI) index. Consequently, for each video sequence, the corresponding models parameters' values of the nearest training video sequence in terms of SI and TI are selected.

For energy measurements, we use a machine with an Intel 2.93 GHz Core 2 Duo processor. As stated earlier, by injecting the encoding time returned by the encoder in Eq. (5), then injecting the result in Eq. (3), we can measure the consumed energy by a given processor for encoding a given video sequence, considering a given configuration ( $FR, QP$ ). The different coefficients of Eq. (3) concerning the processor are available on Intel's website [36]. We report in Table 2 the different tested configurations, as well as the observed prediction error in terms of RMSE of the proposed models in Eqs. (12) and (13).

The distortion is measured in terms of MSE at the output of the encoder. We measure the distortion for the different configurations reported in Table 2. Thereafter, the accuracy of the proposed model in Eq. (16) is evaluated in terms of RMSE, using the measured encoding distortion and the predicted one.

The average prediction error of the proposed models in Eqs. (12), (13) and (16) are, respectively, 7%, 5% and 5.25%, as can be deduced from Table 2 columns  $RMSE_{EE}$ ,  $RMSE_{ED}$  and  $RMSE_{TE}$  respectively. The occurred loss of accuracy of the proposed models, expressed by the increase of the average  $RMSE_{EE}$  (i.e., from 6% to 7%), the average  $RMSE_{ED}$  (i.e., from 4% to 5%) as well as the average  $RMSE_{TE}$  (i.e., from 4% to 5.25%) is mainly due to the considered policy for the selection of the model parameters' values. In fact, in Section 3.1, these values were selected using the curve fitting. While for validation, this selection is done on the basis of the SI and TI information, the parameters' values are not optimal. Nevertheless, the observed prediction errors do not exceed 8%, even if this non-optimal policy is used.

**4.2. Application of the DAEPS procedure**

In this section, we present an application example of the proposed DAEPS procedure for energy consumption minimization under an end-to-end video distortion constraint of 80 in terms of MSE. We consider three identical video sensor nodes deployed at the same distance, of 10 m, of the destination. Each of these nodes

**Table 2**  
Different tested configurations and the prediction errors of the proposed models.

Seq.	Res.	QP	FR	$RMSE_{EE}$ (Eq. (12))	$RMSE_{ED}$ (Eq. (16))	$RMSE_{TE}$ (Eq. (13))
Bus	CIF	20	7.5	7%	6%	5%
News	CIF	34	10	6%	5%	6%
Ice	QCIF	14	15	7%	5%	6%
Fore-man	QCIF	42	12	8%	4%	4%

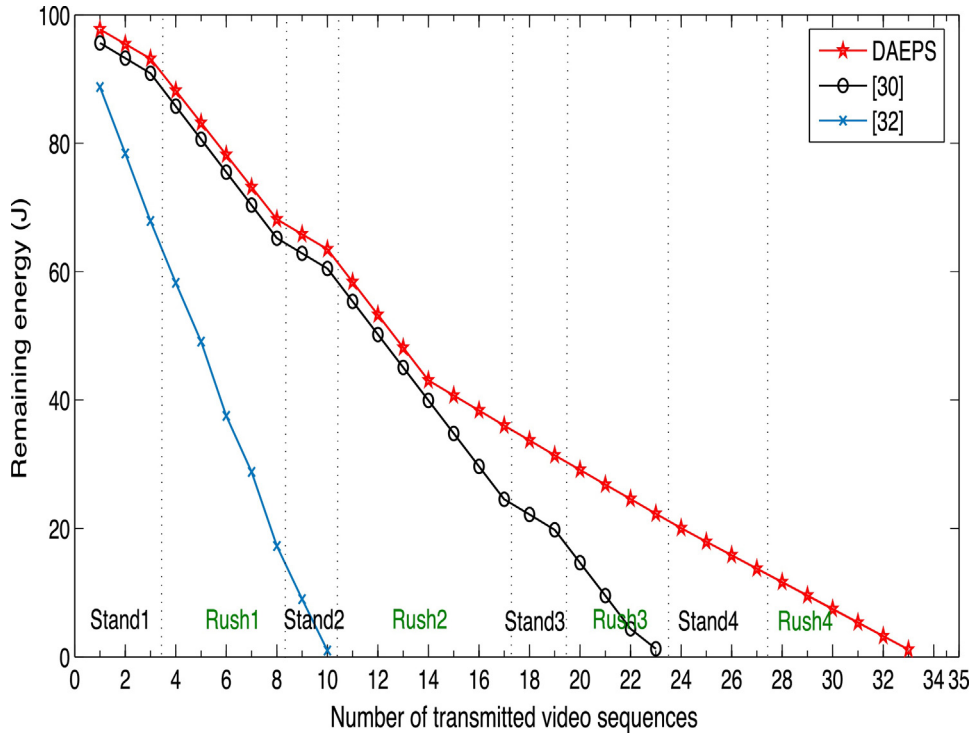


**Fig. 8.** Total energy consumption.

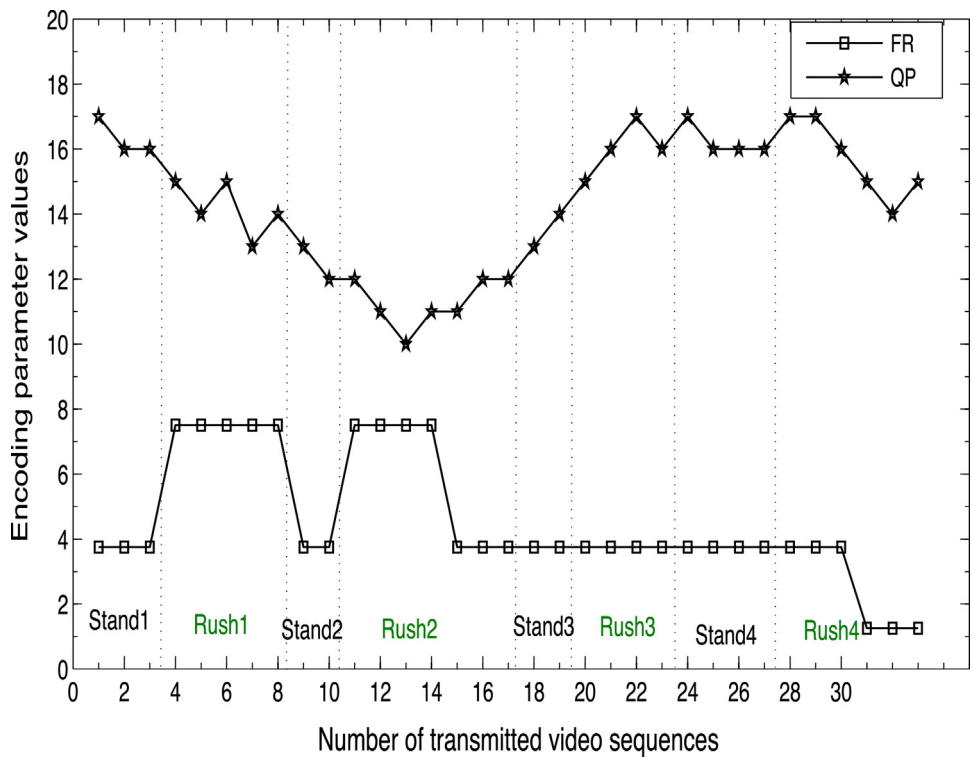


**Fig. 9.** Run-time parameter values.

has an initial energy budget of 100 Joules and implements one of the considered following video encoders. The first is the one presented in [32], the second is presented in [30], while the third is a DAEPS-based encoder. To meet the end-to-end distortion constraint of 80, the QP is set to 14 for both the encoders of [32] and [30]. The FR for standby and rush mode are set to 3.75 and 7.5 respectively, for the encoder presented in [30]. The DAEPS-based encoder adopts the idea of using two modes as in [30] by adopting two different  $FR_{max}$  in each mode, of 3.75 and 7.5 as well. The  $FR_{min}$  is set to 1.75 and  $[QP_{min}, QP_{max}]$  is set to [10,40]. In the following, the LinkState-aware video encoder refers to the scheme of [32] and the energy-efficient video encoder refers to the approach of [30].

The three video sensor nodes encode and transmit the same video sequence with respect to the adopted encoding scheme, as long as there is energy. They are also subject to the same transmission distortions ranging from 10 to 50 in terms of MSE. Hence, we evaluate the performance of the video encoders in terms of the numbers of successively transmitted video sequences, as well as their ability to comply with the required video quality constraint. The video sequence Coastguard is used in QCIF spatial resolution at 30 fps with (SI, TI)=(126,34).

Fig. 8 shows how the energy decreases in each video sensor node, while successively encoding and transmitting the video signal. As can be seen, the remaining energy of the video sensor node using the LinkState-aware video encoder [32], decreases faster than one of the video sensor node implementing the energy-efficient encoder [30], which decreases faster than one of the video sensor node adopting the proposed DAEPS-based video encoding scheme. In fact, the first node was able to successively encode and transmit 10 video sequences, while the second and the third nodes performed that for 23 and 33 video sequences respectively, for the same initial energy budget. We report in Fig. 9 the adopted configuration by the proposed scheme at run-time.

The DAEPS-based encoder outperforms the other video encoders, thanks to its ability to adapt its configuration according to the remaining energy. Hence, when needed, the node decreases the encoder's FR, and progressively increases the QP in order to

decrease the energy consumption and meet the desired quality. In contrast, the LinkState-aware video encoder [32] adapts its configuration with respect to only the current wireless channel state. Furthermore, the energy-efficient [30] video encoder uses a static configuration with no consideration to the current remaining energy. The performed video sensor node lifetime extension using the DAESP-based video encoder is about 2.3 times when compared against the LinkState-aware encoder [32] and about 44% when compared against the energy-efficient encoder [30].

Fig. 10 exposes the behavior of the measured average end-to-end video distortion after concealment. While the energy-efficient video encoder [30] uses constants QP and FR values, the proposed DAEPS-based scheme adapts its configuration according to the actual transmission distortion. In fact, we can observe an interesting behavior of the DAEPS encoder, trying to meet the desired quality constraint by decreasing the encoding distortion when the transmission distortion increases (transmissions 4–20 for example). The awareness of the LinkState-aware video encoder [32] of the current channel state enables it to meet the required end-to-end video quality. On the other hand, unlike the DAEPS-based encoder, the energy-efficient video encoder [30] is not able to comply with the constraint when the transmission distortion increases and exceeds it from transmissions 6–20.

## 5. Conclusion

Video encoding is considered as a challenging task in energy-constrained systems such as the WWSN. We have proposed a dynamic adaptive encoding parameters' values selection (DAEPS) procedure for video node lifetime extension, while meeting a desired end-to-end video quality. This procedure relies on derived empirical models describing the behavior of the consumed energies and the distortions of the encoding and the transmission phases as functions of the quantization parameter (QP) and the frame rate (FR). We first demonstrated through simulations, using a different set of video sequences, the accuracy of the proposed models. Then, we exposed the important lifetime extension, up to 2.3 times,

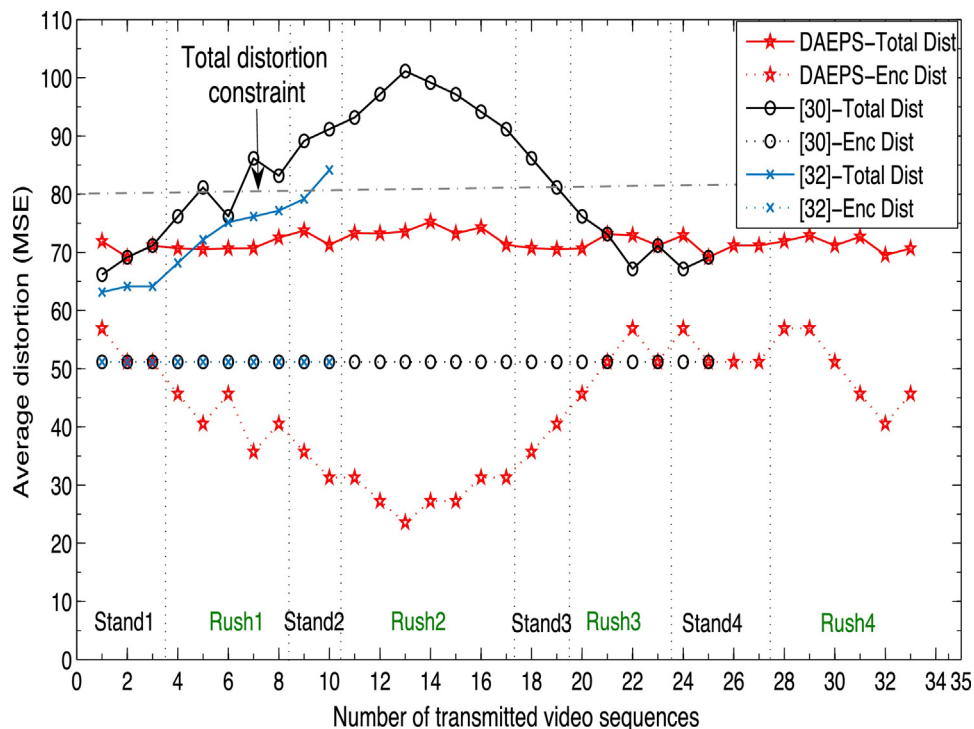


Fig. 10. Average end-to-end distortion after loss concealment.

achieved by the DAEPS-based encoder under an end-to-end video quality constraint, against a LinkState-aware and energy-efficient state-of-the-art video encoders.

As an extension to the presented work, we are working on the implementation of the proposed procedure on a Raspberry Pi 2 based video sensor node. Together, we are working on the consideration of the impact of FR variations on the perceived video quality. One possible way that this the latter could be evaluated empirically instead, is to convert the low-frame-rate video back to the original frame-rate, by repeating frames, then measure the MSE with the original high-frame-rate video, just like distortion is measured. Thus, frame-rate could be interpreted as a form of distortion. Finally, we are looking forward to extending the present study to the High Efficiency Video Coding standard (HEVC/H.265).

## Acknowledgements

This research was supported by the Excellence Fellowships program of the National Center for Scientific and Technical Research (CNRST) of Morocco (G01/003) and the Franco-Moroccan cooperation program in STICs for the research project "RECIF".

## References

- [1] H.M.A. Fahmy, *Wireless Sensor Networks: Concepts, Applications, Experimentation and Analysis*, no. 1 in *Signals and Communication Technology*, Springer, 2016.
- [2] L.M. Borges, F.J. Velez, A.S. Lebres, Survey on the characterization and classification of wireless sensor network applications, *IEEE Commun. Surv. Tutor.* 16 (4) (2014) 1860–1890, <http://dx.doi.org/10.1109/COMST.2014.2320073>.
- [3] N.A. Pantazis, S.A. Nikolidakis, D.D. Vergados, Energy-efficient routing protocols in wireless sensor networks: a survey, *IEEE Commun. Surv. Tutor.* 15 (2) (2013) 551–591, <http://dx.doi.org/10.1109/SURV.2012.062612.00084>.
- [4] M.A. Kafi, D. Djenouri, J. Ben-Othman, N. Badache, Congestion control protocols in wireless sensor networks: a survey, *IEEE Commun. Surv. Tutor.* 16 (3) (2014) 1369–1390, <http://dx.doi.org/10.1109/SURV.2014.021714.00123>.
- [5] I.F. Akyildiz, T. Melodia, K.R. Chowdury, Wireless multimedia sensor networks: a survey, *IEEE Wirel. Commun.* 14 (6) (2007) 32–39, <http://dx.doi.org/10.1109/MWC.2007.4407225>.
- [6] S. Soro, W. Heinzelman, A survey of visual sensor networks, *Adv. Multimed.* (2009), <http://dx.doi.org/10.1155/2009/640386>.
- [7] X. Liu, A survey on wireless camera sensor networks, in: *Frontier and Future Development of Information Technology in Medicine and Education*, Vol. 269 of *Lecture Notes in Electrical Engineering*, Springer Netherlands, 2014, pp. 1085–1094, <http://dx.doi.org/10.1007/978-94-007-7618-0.106>.
- [8] F.G. Yap, H.-H. Yen, A survey on sensor coverage and visual data capturing/processing/transmission in wireless visual sensor networks, *Sensors* 14 (2) (2014) 3506–3527, <http://dx.doi.org/10.3390/s140203506>.
- [9] J.J. Ahmad, H.A. Khan, S.A. Khayam, Energy efficient video compression for wireless sensor networks, 43rd Annual Conference on Information Sciences and Systems (CISS) (2009) 629–634, <http://dx.doi.org/10.1109/CISS.2009.5054795>.
- [10] *Advanced video coding for generic audiovisual services*, ITU-T Recommendation H.264, 2017.
- [11] O. Alaoui-Fdili, Y. Fakhri, P. Corlay, F.X. Coudoux, D. Aboutajdine, Energy consumption analysis and modelling of a H. 264/AVC intra-only based encoder dedicated to WVSNS, IEEE International Conference on Image Processing (ICIP) (2014) 1189–1193, <http://dx.doi.org/10.1109/ICIP.2014.7025237>.
- [12] LILIN IPD2220ES, <http://www.ttsys.com/pdf/RFID/IPD2220ES-EN.TTS.v4.pdf> (accessed 26.11.16).
- [13] O. Alaoui-Fdili, F.-X. Coudoux, Y. Fakhri, P. Corlay, D. Aboutajdine, Energy-efficient joint video encoding and transmission framework for wvsns, in: *Multimedia Tools and Applications*, 2017, <http://dx.doi.org/10.1007/s11042-017-4904-6>.
- [14] R. Anane, R. Bouallegue, K. Raouf, Medium access control (MAC) protocols for wireless sensor network: an energy aware survey, in: *Mediterranean Conference on Information & Communication Technologies (MedICT)*, Lecture Notes in Electrical Engineering, Springer International Publishing, 2016, pp. 561–569, <http://dx.doi.org/10.1007/978-3-319-30301-7.60>.
- [15] V.-T. Nguyen, M. Gautier, O. Berder, FTA-MAC: fast traffic adaptive energy efficient mac protocol for wireless sensor networks, in: *International Conference on Cognitive Radio Oriented Wireless Networks (CROWNCOM)*, Springer, 2016, pp. 207–219, <http://dx.doi.org/10.1007/978-3-319-40352-6.17>.
- [16] M. Sha, G. Hackmann, C. Lu, Energy-efficient low power listening for wireless sensor networks in noisy environments, in: *12th international conference on Information processing in sensor networks (IPSN)*, ACM, 2013, pp. 277–288, <http://dx.doi.org/10.1145/2461381.2461415>.
- [17] S. Cui, A.J. Goldsmith, A. Bahai, Energy-constrained modulation optimization, *IEEE Trans. wirel. Commun.* 4 (5) (2005) 2349–2360, <http://dx.doi.org/10.1109/TWC.2005.853882>.
- [18] Q. Chen, M.C. Gursoy, Energy-efficient modulation design for reliable communication in wireless networks, 43rd Annual Conference on Information Sciences and Systems (CISS) (2009) 811–816, <http://dx.doi.org/10.1109/CISS.2009.5054829>.
- [19] S.E. Abdellaoui, M. Debbah, Y. Fakhri, D. Aboutajdine, Increasing network lifetime in an energy-constrained wireless sensor network, *Int. J. Sens. Netw.* 13 (1) (2013) 44–56, <http://dx.doi.org/10.1504/IJSNET.2013.052730>.
- [20] S. Ulukus, A. Yener, E. Erkip, O. Simeone, M. Zorzi, P. Grover, K. Huang, Energy harvesting wireless communications: a review of recent advances, *IEEE J. Select. Areas Commun.* 33 (3) (2015) 360–381, <http://dx.doi.org/10.1109/JSAC.2015.2391531>.
- [21] D. Feng, C. Jiang, G. Lim, L.J. Cimini, G. Feng, G.Y. Li, A survey of energy-efficient wireless communications, *IEEE Commun. Surv. Tutor.* 15 (1) (2013) 167–178, <http://dx.doi.org/10.1109/SURV.2012.020212.00049>.
- [22] T. Kim, I.H. Kim, Y. Sun, Z. Jin, Physical layer and medium access control design in energy efficient sensor networks: an overview, *IEEE Trans. Ind. Inform.* 11 (1) (2015) 2–15, <http://dx.doi.org/10.1109/TII.2014.2379511>.
- [23] W. Heinzelman, A. Chandrakasan, H. Balakrishnan, Energy-efficient communication protocol for wireless microsensor networks, *The Annual Hawaii International Conference on System Sciences*, vol. 2 (2000) 10, <http://dx.doi.org/10.1109/HICSS.2000.926982>.
- [24] X. Liu, A survey on clustering routing protocols in wireless sensor networks, *Sensors* 12 (8) (2012) 11113, <http://dx.doi.org/10.3390/s120811113>.
- [25] A.E. Zonouz, L. Xing, V.M. Vokkarane, Y. Sun, Hybrid wireless sensor networks: a reliability, cost and energy-aware approach, *IET Wirel. Sens. Syst.* 6 (2) (2016) 42–48, <http://dx.doi.org/10.1049/iet-wss.2014.0131>.
- [26] J. Yan, M. Zhou, Z. Ding, Recent advances in energy-efficient routing protocols for wireless sensor networks: a review, *IEEE Access* 4 (2016) 5673–5686, <http://dx.doi.org/10.1109/ACCESS.2016.2598719>.
- [27] T. Ma, M. Hempel, D. Peng, H. Sharif, A survey of energy-efficient compression and communication techniques for multimedia in resource constrained systems, *IEEE Commun. Surv. Tutor.* 15 (3) (2013) 963–972, <http://dx.doi.org/10.1109/SURV.2012.060912.00149>.
- [28] T. Sheltami, M. Musaddiq, E. Shakhshuki, Data compression techniques in wireless sensor networks, *Fut. Gener. Comput. Syst.* 64 (2016) 151–162, <http://dx.doi.org/10.1016/j.future.2016.01.015>.
- [29] D. Rui, W. Pu, I. Akyildiz, Correlation-aware QoS routing with differential coding for wireless video sensor networks, *IEEE Trans. Multimed.* 14 (5) (2012) 1469–1479, <http://dx.doi.org/10.1109/TMM.2012.2194992>.
- [30] O. Alaoui-Fdili, F. Coudoux, Y. Fakhri, P. Corlay, D. Aboutajdine, Energy efficient adaptive video compression scheme for WVSNS, *21st European Signal Processing Conference (EUSIPCO 2013)* (2013) 1–5.
- [31] A.A. Youssif, A.Z. Ghalwash, M.E.E.D.A. El, et al., ACWSN: an adaptive cross layer framework for video transmission over wireless sensor networks, *Wirel. Netw.* 21 (8) (2015) 1–18, <http://dx.doi.org/10.1007/s11276-015-0939-7>.
- [32] M.E.E.D. Abd El Kader, A.A.A. Youssif, A.Z. Ghalwash, Energy aware and adaptive cross-layer scheme for video transmission over wireless sensor networks, *IEEE Sens. J.* 16 (21) (2016) 7792–7802, <http://dx.doi.org/10.1109/JSEN.2016.2601258>.
- [33] A.A. Ahmed, An optimal complexity h. 264/avc encoding for video streaming over next generation of wireless multimedia sensor networks, *Signal Image Video Process.* 10 (6) (2016) 1143–1150, <http://dx.doi.org/10.1007/s11760-016-0870-0>.
- [34] *Subjective video quality assessment methods for multimedia applications*, ITU-T RECOMMENDATION, 1999.
- [35] P.S. Boluk, S. Baydere, A.E. Harmanci, Perceptual quality-based image communication service framework for wireless sensor networks, *Wirel. Commun. Mobile Comput.* 14 (1) (2011) 1–18, <http://dx.doi.org/10.1002/wcm.1218>.
- [36] Intel core2 duo processor, <http://support.intel.co.jp/pressroom/kits/core2duo/> (accessed 07.11.16).